Journal of Scientific Exploration, Vol. 25, No. 2, pp. 237–264, 2011 0892-3310/11

RESEARCH

Measurement Controls in Anomalies Research

Walter E. Dibble, Jr.

William A. Tiller

Submitted 9/16/10; Accepted 2/1/11

Abstract—Members of the Society for Scientific Exploration have expressed considerable concern regarding proper control measures in research of anomalies (subtle energy research, etc.). This is quite proper and deserves some comment from us since the topic applies so well to the work we are conducting in "conditioned spaces." Also, the need by researchers for good "anomaly detectors" is paramount and is intimately connected to the search for good controls. Both issues are addressed in this communication.

The Fundamental Equation

The basic equation we have been using for years in our IHD (intention host device) to evaluate all anomalous results from the research we have been conducting is as follows (Tiller, 2007, 2010a),

$$Q_M = Q_e + \alpha_{eff} Q_m \qquad (1)$$

where $\alpha_{eff}Q_m$ is usually a time-dependent function of sigmoidal or exponential form (a front-clipped sigmoid). In this zeroth-order approximation equation, the quantity Q_M represents a measured value derived from using **any** kind of sensor/detector. The quantity Q_e represents a measured value from a sensor/detector that is not affected in any way by any anomaly-producing factor or influence. The quantity Q_e is a measurement result that is normally produced by conventional equipment in conventional laboratories by conventional scientists/technicians. On the other hand, Q_m represents something very different. This quantity represents a component of any measurement, Q_M which **is** affected by anomaly-producing factors or influences.

In our IHD work (see Appendix 1), we are talking about two uniquely different domains of nature. The first domain is the domain of the conventional

(solely our distance–time reference frame), and the second domain is the domain where, relative to the first domain, anomalies are detected. The coefficient, α_{eff}, is the quantity that connects the two domains; hence, it is a time-dependent coupling coefficient. When this coefficient is zero, $Q_M = Q_e$ and no anomalies are detected (anomalies may not be detected even when α_{eff} is non-zero, if the sensor used cannot detect them, see below). Our fundamental assumption/axiom is that, for conventional laboratories using conventional equipment operated by conventional scientists/technicians, $\alpha_{eff} = 0$. For any "real" laboratory, this condition will not precisely hold, but this is the ideal condition for any control laboratory. Based on our experience, control laboratories are to be valued for their capability for producing measurement values consistent with the Q_e component in Equation 1.

Real Experimental Measurements

For any real measurements, as opposed to the ideal condition mentioned above, Q_M may have a Q_m component as well as a Q_e component. In our experience with "conditioned" spaces, there may be a variety of partially coupled states ($\alpha_{eff} \neq 0$) to consider. Just how do we, working in such a partially coupled environment, sort these two out? This is really where the rubber hits the road in any serious anomaly research.

The primary thermodynamic intensive variables of our normal reality are temperature, pressure, and composition. Anomalies can affect any of these quantities, but we have chosen to focus on temperature and composition. A variety of sensors are available to measure temperature and composition. For all of these, what is really measured is some quantity that is a function of temperature or the composition component of interest. Thus, there is much, much more involved than just measuring temperature or composition in the design and construction of each particular sensor. Each of the measurement components, individually, can be affected by anomalies. What we usually observe is a sum total effect. Ultimately, the individual component contributions to an anomalous measurement will need to be sorted out as well.

That being said, let us examine some real applications that allow us to address the control issue more completely. A composition sensor that we like to use is a pH-electrode. This sensor has a number of components but can, with proper use, yield an accurate value for the pH of an aqueous solution (Pajunen, Purnell, Dibble, & Tiller, 2009). For the pH application, Equation 1 yields

$$pH_M = pH_{U(1)} + \alpha'_{eff} pH_m. \quad (2)$$

In this expression of Equation 1, we have just replaced Q_M and Q_m with pH_M and pH_m, respectively. In this case, $pH_{U(1)}$ is a value of pH unaffected by any anomaly-producing factor or influence, consistent with Equation 1. For the definition of any kind of anomaly using this sensor, we are interested in the value of pH_M minus $pH_{U(1)}$. This value we sometimes refer to as ΔpH which equals $\alpha'_{eff}pH_m$. We use α'_{eff} to designate a different coupling coefficient than the generic one used in Equation 1.

The remaining issue is how to determine a value for $pH_{U(1)}$ that any measurement of ΔpH depends on. This can be done by the choice of an appropriate measurement medium. Ideally this is a medium for which one can independently calculate a pH value as a function of temperature. For a variety of reasons (see Appendix 2), we chose to use pure water in equilibrium with air as our medium (Tiller, Dibble, & Kohane, 2001). For this particular medium, the equilibrium pH can be calculated as a function of temperature using only thermodynamic data (Appendix 2). This data includes equilibrium constants measured reproducibly in a number of different laboratories. The fundamental assumption used here is that these equilibrium constants were measured using conventional equipment operated by conventional scientists/technicians in laboratories where $\alpha'_{eff} = 0$. Our results are only as good as this assumption, but we assert that it is a good one.

So what constitutes a control here? In this case, the control is the thermodynamic data reported from a number of different laboratories which we assume are located in spaces where $\alpha'_{eff} = 0$. The thermodynamic data is usually reported in compendia compiled using certain standards. If a lab were partially coupled ($\alpha'_{eff} \neq 0$), it is less likely that results from that lab would compare well with uncoupled lab results and such results would not as likely be included in the various compendia of thermodynamic data.

Real Anomaly Examples Using the pH-Sensor

In the case of Equation 2, an anomaly is defined when there is a marked difference between the pH_M and $pH_{U(1)}$ values. However, there can be more to it than that as illustrated by some recent examples. In Figure 1 we plot pH results from Conditioned Space A where anomalies of various sorts are present. The lower curve is the pH calculated from thermodynamic data as a function of the measured water temperature (see Appendix 2). The wavy nature of these curves is due to the diurnal temperature variation at this site. The measured temperature dependence of pH_M is much higher than it should be (the ratio $pH_M/pH_{U(1)}$). To illustrate, if we take the ratio of pH amplitudes (trough to peak) between hours 285 to 293, we find it to be 0.21/0.033, or about 6.4. The overall rise in pH_M is also six times what it should be for the overall temperature increase. From the temperature low at hour 168 to the high at hour 293, $pH_{U(1)}$ increases only from

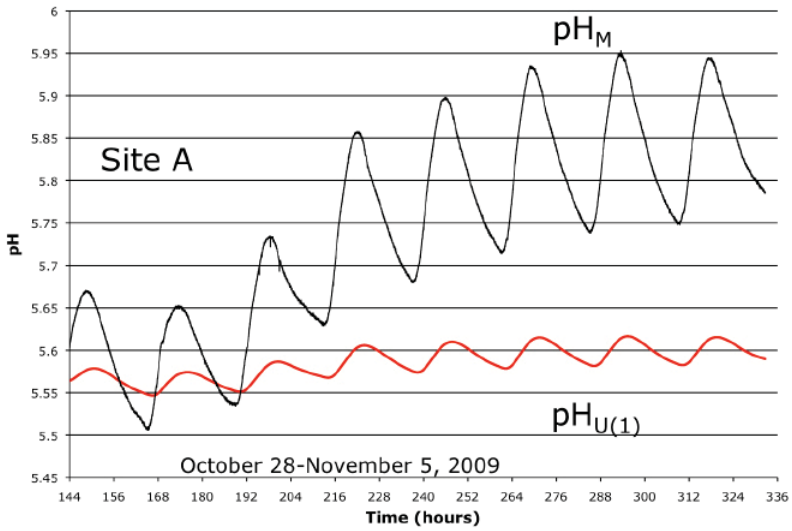

Figure 1. pH vs. time for site A (Equation 2 defines pH_M).

5.545 to 5.614, or about 0.07 pH units. On the other hand, pH_M increases 0.44 pH units over the same time interval (from 5.51 to 5.95), for a ratio of pH_M/$pH_{U(1)}$ of 6.3. Such amplification (more than six times!) is highly anomalous. Figure 2 shows the opposite case in another conditioned space. Here, the measured pH varies with temperature about 1/3 as much as it should. (It is also not exactly in phase with temperature, but that is another anomaly story.) Thus, this pH-temperature dependence can be considerably greater or less than what it should be compared to a control (that is in conditioned, partially coupled spaces where $\alpha'_{eff} \neq 0$). Figure 1 and Figure 2 represent just a small sample of the kinds of anomalies that can be revealed in conditioned spaces using this particular type of sensor. In these cases, the control using thermodynamic data is clearly very useful.

Temperature Sensor Controls and Detectors

Temperature sensors can also be used in anomaly research but the controls are different and more difficult to define. From Equation 1, we have, for a temperature sensor, the following analogous result:

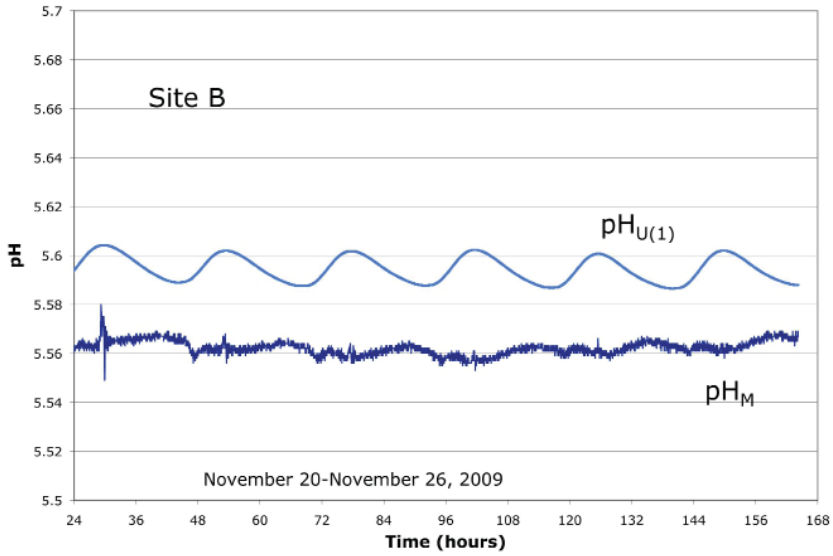

Figure 2. pH vs. time for site B, November 2009.

$$T_M = T_e + \alpha''_{eff} T_m. \quad (3)$$

In this case, a different coupling coefficient, α''_{eff}, is designated so as to not confuse it with the others. Again, we have the problem of separating out T_e from an actual temperature, T_M, measured using various kinds of temperature sensors.

The practical solution to this problem is to look for a temperature sensor that does not respond to any anomaly-producing factor or influence. In other words, we look first for a good control sensor that will allow us to determine an accurate value for T_e only. On the other hand, we are also looking for a temperature sensor that responds well to our anomaly-producing factors. This equation, therefore, demonstrates that a good detector of temperature anomalies involves both a sensor that can be used as a control (measures T_e accurately) and one that responds to T_m (i.e. two different sensors). Once these two sensors have been identified, a quantitative picture of a temperature anomaly can be revealed by subtracting T_e from T_M.

We are fortunate in that we can create spaces that have values of $\alpha_{eff} \neq 0$ for the space (two examples are shown in Figure 1 and Figure 2). This allows us to test a variety of temperature sensors to see how they respond in such an

environment. Research on these sensors is in progress. We have recently been successful, using temperature calibration techniques, in identifying the types and kinds of temperature sensors necessary to satisfy the constraints of Equation 3. Also, since pH_M is a function of the measured temperature, there is also a component T_m that will affect the pH measurement as well. Thus, we have an important dual purpose for performing temperature sensor experiments in conditioned spaces.

Entanglement Issues Involved in Defining Controls

From the foregoing, it can be seen that controls can take different forms in experiments on anomalies. One example was the use of thermodynamic data and another was the identification of sensors that do not respond at all to anomaly-producing factors. A different control needing discussion is the experimental control space. In such a space, α_{eff} in Equation 1 is zero and no anomalies are observed. In our experience in trying to locate and utilize such spaces, we found that serious spatial and sometimes temporal entanglement occurs with our "conditioned" spaces rendering such spaces useless (as controls). This effect (Tiller, Dibble, & Fandel, 2005) shows how macroscopic entanglement must be addressed in any serious anomaly research (Tiller, 2010b:508–510). We are also searching for a means to "erase" space "conditioning" and find that to do so requires much more understanding of all the processes involved than we currently possess.

Spatial Entanglement

Early on in our research involving conditioned spaces produced by operating intention-imprinted electrical devices (IIEDs) (Tiller, Dibble, & Kohane, 2001, Tiller, Dibble, & Fandel, 2005, Tiller, 2007), we found that it was not possible to cleanly isolate imprinted devices from un-imprinted devices (UEDs). After a period of time, the UEDs also became imprinted to a certain extent. This was our first introduction to macroscopic entanglement. We experimented with various types of shielding methods, also with varying degrees of success. It appeared to us, after some experience with these kinds of devices, that some entanglement resulted from electromagnetic carrier wave sources. As a result, we designed some shielding to block a portion of this. However, the interesting part of this information entanglement could not be blocked.

A Recent Case Study

A recent example of such entanglement using the pH-sensor detection system involved monitoring the pH of highly purified water simultaneously at sites about 90 miles apart. One site, C, is in the mountains northeast of Phoenix,

Arizona, in a very small shed at an elevation of 5,000 feet with power but no atmospheric controls (no heating or A/C). The other site, D, is in an industrial area of Phoenix in a large industrial building with A/C capability. We were running similar IIEDs at both sites, a unique feature we consider to be the source of the entanglement between these two sites.

From Equation 2, we defined ΔpH (= $pH_M - pH_{U(1)}$) to be a value we could use as an indicator of conditioned spaces or spaces where anomalies are detected. We converted this value to an excess energy (excess thermodynamic free energy) (Tiller, Dibble, & Fandel, 2005, Tiller, 2007) with energy units (milli-electron volts) that everyone is familiar with (ΔpH is unfamiliar to most as an indicator quantity). This value we have designated as δG^*_{H+}, and it can be thought of as the energy equivalent of the ΔpH values derived from Equation 2. The subscript H^+ refers to the fact that we derive this δG^*_{H+} value for the aqueous hydrogen ion from pH measurements. Using this excess free energy, we plot in Figure 3 how weekly averages of this δG^*_{H+} value correlate for the two sites C and D. As can be seen in Figure 3, there was not a very high correlation initially, but after a short time a strong negative correlation developed. This correlation abruptly shifted to a strong positive value after about six weeks. The high correlations indicate a high degree of entanglement between these widely separated sites. The change in the sign of correlations such as these appears to

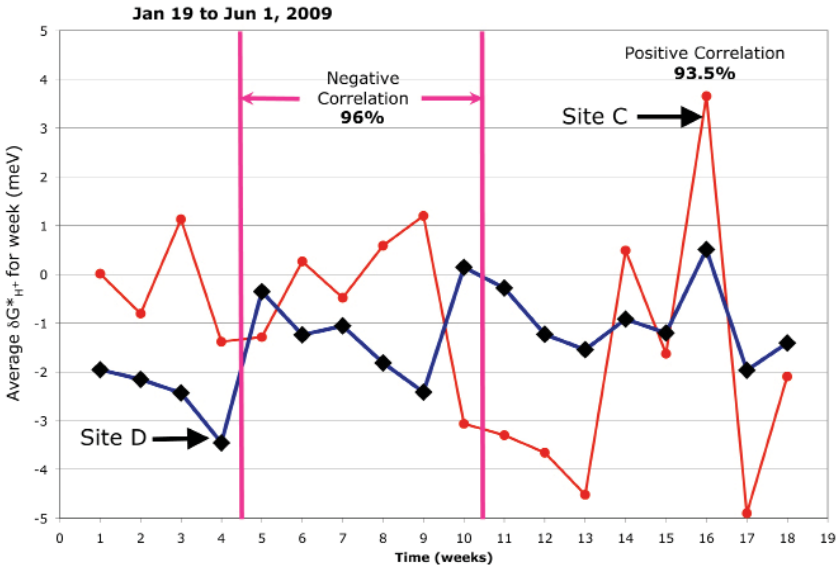

Figure 3. Average weekly values of δG^*_{H+} plotted vs. time.

happen often in conditioned spaces as a result of macroscopic, room-temperature entanglement. The mechanism producing these correlation sign changes is presently unknown and probably relates to anomaly-producing factors not understood fully. However, the existence of the correlation sign changing strongly suggests a non-physical origin.

Air Temperature Entanglement

In Figure 1 the scale is insufficient to reveal that the two pH values displayed are not precisely in phase (pH_M and $pH_{U(1)}$). However, on closer inspection this becomes clearer. A better example of this phenomenon is given in Figure 4. In this system the air temperature changes diurnally as a result of the solar heating cycle. Changes in air temperature are transmitted to the water from the air via heat flow. Because of finite heat flow rates and large differences in specific heat per unit volume, the change in water temperature lags significantly behind the change in air temperature, as can be observed in Figure 4.

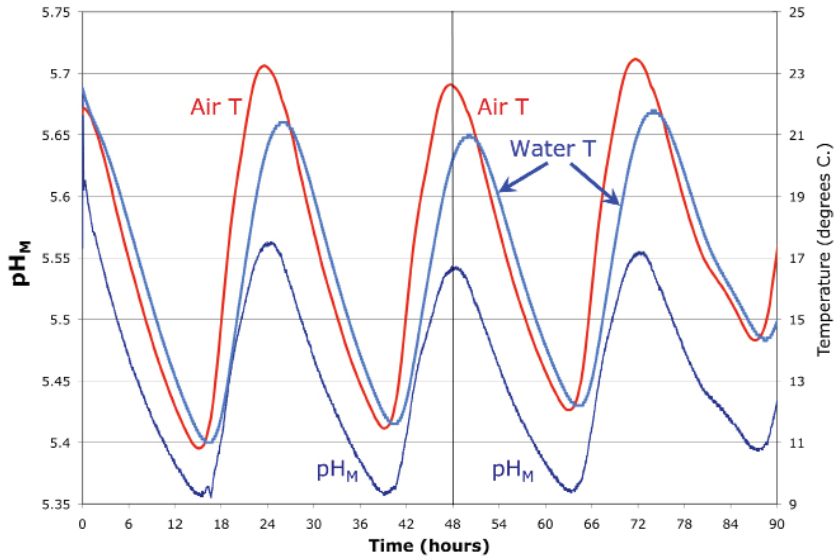

Figure 4. pH and temperature vs. time at site A (April 22–26, 2010).

Table 1 shows the time differences between the highs and lows in air and water temperatures and the corresponding highs and lows in pH as depicted in Figure 4. The pH extremes all occur, in time, between the extremes in air

TABLE 1
Time Differences (Δt) in Minutes between Extrema in pH and Extrema for Air vs. Water Temperatures (from Figure 4, note the sign differences)

Figure 4 Extremum	Δt [pH(t) – Air T(t)]	Δt [pH(t) – Water T(t)]
Low 1	+13	−64
Low 2	+1	−80
Low 3	+14	−60
Low 4	+18	−57
High 1	+39	−93
High 2	+33	−115
High 3	+28	−112

and water temperature. This is shown in Table 1, where the time difference between the pH extremes and the air temperature extremes (time of pH extreme minus time of air temperature extreme in minutes) is positive, meaning that the air temperature extremes lead the pH extremes, in time. On the other hand, the pH extremes clearly lead the extremes in water temperature (negative time difference). As revealed in Table 1, the pH extremes are all significantly closer, in time, to the air temperature. Also these differences vary depending on whether the extremum is a high or a low. This effect needs further study and evaluation.

Correlation coefficients calculated for the 90-hour time period shown in Figure 4 indicate a similar out-of-phase condition. The pH is about 97% correlated with the air temperature and only 90% correlated to water temperature. This situation is reversed in conventional spaces where the pH is closely correlated with water temperature. In a normal space, the air temperature leads the water temperature (as it does in this case) and the pH change correlates with the water temperature change only ($pH = f(T_{water})$ and $pH \neq f(T_{air})$. The water temperature will always be correlated with the air temperature (heat flows from the air to the water and out again, forced by variation in air temperature). Thus, the pH correlation with the air temperature is the significant (anomalous) correlation here.

The pH-electrode is totally submersed in water (about one quarter liter) near the center of the container. We know from thermodynamics how the water

pH varies with the water temperature. However, from Figure 4, we see that the pH is much more in-phase with the air temperature, not the water temperature! When every peak or trough in temperature is examined carefully, as revealed in Table 1, the extremes in pH align much better with those of the air temperature. There is much less of a time lag between peaks and troughs in air temperature and pH. This pH correlation with air temperature does not happen in conventional, un-conditioned spaces where the pH is a function of water temperature **not** air temperature. At site A, the type of phase shifts that are so visually compelling in Figure 4 have been measured for more than 7,000 hours. At another "conditioned" site (roughly 40 meters away), less pronounced but quantitatively significant correlations between the pH and air temperature have been measured for more than 40,000 hours.

We see such pH behavior commonly in spaces conditioned by IIEDs, and it is one of the hallmarks of what we call space conditioning. Figure 4 is one of the better examples of the phenomenon. What this behavior reveals is one aspect of how macroscopic entanglement manifests in such spaces. In this case, the pH of water becomes strongly entangled with the air temperature and is one example of how "action at a distance" via entanglement can work in conditioned spaces.

Discussion

Equation 1 reveals just where the control comes in to an approximate evaluation of anomalous phenomena. There also exists in the expression a term defining where the anomalous component may enter. However, nature is more complicated than a simple expression such as Equation 1, and the existence of macroscopic entanglement demonstrates the importance of the further work needed to add other elements, something beyond the scope of this paper.

It seems clear from these few examples how difficult it becomes to define a "control" space or laboratory in environments that are specifically created to manifest such anomalous behavior. One problem occurs when macroscopic entanglement is established in such environments. The air temperature entanglement described above makes the definition of an appropriate temperature control difficult. If the pH does not vary with the water temperature but instead shifts to varying with the air temperature (Figure 4), then shouldn't one be using the air temperature to define $pH_{U(1)}$ in such cases? The question of what temperature to use goes back to Equation 2 and Equation 3. The measured pH is a function of temperature as well as α'_{eff} for the pH measurement. The measured temperature is a function of α''_{eff} for the temperature measurement. All these quantities are entangled in a very complex way that has yet to be fully understood.

We have measured temperature using a variety of sensors in a conditioned space (red-spirit, mercury, thermister, and thermocouple) and find that, in such

spaces, the difference in temperatures between sensors is invariably greater than in other "more conventional" spaces. The search for the best temperature control in such spaces has yielded another reliable and exciting subtle energy detection system.

Where Does Equation 1 Come From?

By now, we hope the reader of this paper has come to appreciate that there are practical uses for an expression such as Equation 1 to evaluate anomalous phenomena, at least for the IHD (Intention-host Device) experiments. Not the least of these is establishing a basis for defining what the controls are. Now we would like to show some of the theoretical background used in defining this expression that, hopefully, will further suggest the richness of the approach that can be used.

About 13 years ago, one of us proposed that science consider the utility of using a specific duplex space RF consisting of two, **reciprocal**, four-dimensional subspaces, one of which is distance/time (Tiller, 1997:54–100). The reciprocal domain subspace is a frequency domain that can be linked to the spacetime subspace via α_{eff}. The origin of Equation 1 comes from the mathematics presented first in Chapters 7 and 8 of Tiller, Dibble, and Kohane (2001).

The very important mathematical property of a duplex space consisting of two reciprocal subspaces, is that a unique quality functioning in one subspace has an equilibrium quantitative connection to its conjugate quality in the reciprocal subspace via a type of equilibrium Fourier transform (FT) pair relationship; such a pair of equations can be generalized to any number of dimensions as shown in Tiller, Dibble, and Kohane (2001:304–305).

This means that if we calculate a mathematical description of a quality in one subspace, one can, in principle, calculate the equilibrium conjugate quality in the other subspace. However, in our duplex space case, a coupling substance must be present to allow a substance quality of one subspace to actually interact with the conjugate substance quality of the reciprocal subspace substance. We thus need to define and name this coupling substance which we label "deltrons." Without this kind of deltron coupling, the thermodynamic equilibrium between the two uniquely different kinds of substance could never be achieved (Tiller & Dibble, 2007). To begin to illustrate this interaction, we use Figure 5. The top portion shows in (b) a Gaussian-shaped packet of R-space substance, $g(k_x)$, while (a) shows an FT wave packet of Gaussian envelope shape in spacetime (D-space). The bottom portion of Figure 5 shows in (c) a spherical particle of D-space substance, while (d) shows its $g(k_rR)/2\pi R^2$ analogue in reciprocal space. Here, items (b) and (c) are substances while items (a) and (d) are only calculated ghosts (virtual substances). However, when sufficient deltrons are added, the substances a and b plus c and d can interact with each other (provided

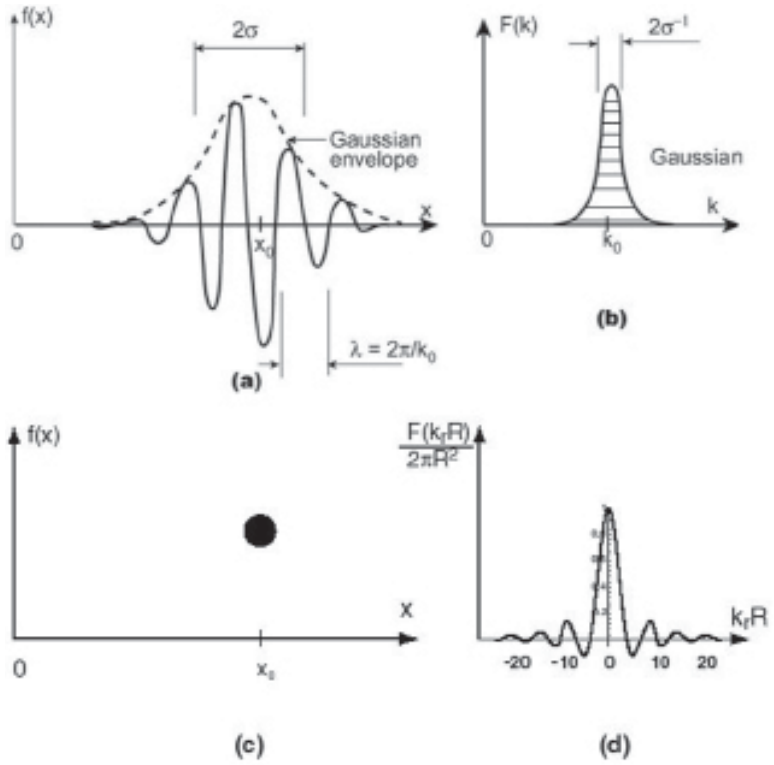

Figure 5. Classical Fourier Transform: D-space/R-space pairs
(a) a "ghost" calculated D-space wavegroup for
(b) a real R-space, Gaussian substance packet,
(c) a real D-space 2-D particle of radius R, and
(d) its "ghost" calculated R-space conjugate wavegroup.
For an atom, one would choose R ~ 10^{-8} cm.

we use the same geometrical shapes), and one has functional de Broglie particle/pilot wave systems (White Paper V, http://www.tiller.org) in both subspaces that can seek thermodynamic equilibrium between its distinguishable parts.

In our mathematical formalism, the quantitative relationship between the interacting substances of the two, reciprocal subspaces are given in one dimension, where s = any of x,y,z,t, by

$$C_{\delta}(s,k_s)f(s) = \frac{1}{(2\pi)^{1/2}} \int_{-\infty}^{\infty} g(k_s)e^{-i2\pi s \bullet k_s} dk_s \qquad (4a)$$

and

$$g(k_s) = \frac{1}{(2\pi)^{1/2}} \int_{-\infty}^{\infty} C_{\delta}(s,k_s) f(s) e^{i2\pi s \cdot k_s} ds \qquad (4b)$$

This pair of equations is importantly different from the standard FT pair because of our presently unknown deltron activation function, $C_{\delta}(s,k_s)$, which one might consider expanding as an orthonormal set of functions in both s and k_s. In the zeroth-order approximation, only the constant term in C_{δ} is retained, and this has been labeled α_{eff} in Equation 1.

It should also be understood by the reader that if one substitutes $Q_e(t)$ for f(s) and t for s in Equation 4b,

$$Q_m = \int_{R-space} I(k_t)dk_t \quad and\ I(k_t) = g(k_t)g^*(k_t) \qquad (5)$$

where $I(k_t)$ is the intensity and g* is the complex conjugate of g. Further, although Q_e is sometimes a mathematical scalar, Q_m is always a mathematical vector or a tensor. Appendix 3 illustrates how Equation 4 and Equation 5 are utilized with $pH_M(t)$ experimental data to gain useful insights on our general IHD research.

A Further Word About Anomalies, Anomalous Phenomena, and the Working Hypothesis Reference Frames Constructed To Model Them

We have been engaged in measuring a variety of anomalous physical–chemical behavior in spaces "conditioned" by an IHD (Intention-Host Device). This measured behavior is well-defined with such large effect-size, it is quite beyond the consciousness-correlated physical phenomena defined by Jahn and Dunne (2008) that require evaluation using rigorous statistical methods. For the most part, the details regarding the IHD and its operation are beyond the scope of this paper. We are primarily interested in categorizing and understanding the anomalies produced by this device in communications such as this. This general approach would apply to anomalies produced by a broad range of other devices with similar (albeit mysterious) operating principles. As a first step, we have generated Equation 1 from a zeroth-order approximation of a more general theory that allows us to begin the evaluation process. We think that others engaged in anomalies research may be able to make some use of this approach in their work.

Anomalies we have identified would be considered the "Not-OK" or "Sleeping" variety as defined by Sturrock (2007). Atmanspacher (2009) would probably consider them to be his "Anomalies in No-Man's Land." These characterizations illustrate some of the terminology that indicates anomalies that are outside conventionally accepted theoretical understanding. However, we prefer to divide anomalies of the types discussed by Sturrock (2007), Jahn and Dunne (2008), and Atmanspacher (2009) into two much more basic and meaningful groups.

Group A Anomalies. Group A anomalies would be those that can be considered to be spacetime anomalies that are accessible to spacetime models including quantum mechanics (QM). If the anomaly can ultimately (if not at the present time) be explained using QM, then it is a Group A anomaly. These phenomena can normally be described using potential functions that are space and time dependent.

Group B Anomalies. Group B anomalies would include those that exist outside spacetime and that are not accessible to models grounded in spacetime such as QM. Group B anomalies cannot be explained using QM, and they cannot be described using potential functions that are space and time dependent.

We very much appreciate the comments on this issue by Werbos (2001) that definitely apply to the Group B-type anomalies:

> Many people . . . have expressed hope that quantum mechanics might explain things like remote viewing or like the collective unconscious of Jung—wild, crazy things. I would like to point out that no form of quantum mechanics can explain something like remote viewing. It doesn't matter whether you take

> Bohmian or my kind or Schwinger's kind or Copenhagen. . . . because all these different forms of quantum mechanics produce about the same quantum electrodynamics. . . . they yield the same predictions, essentially, for the case of quantum electrodynamics (QED). If you consider electrodynamics, that is not enough to generate remote viewing. We know what is possible with QED. The world has spent billions of dollars trying to use QED in the military to see things far away. We cannot do it. So if you want to explain strange things like remote viewing, the only way is by assuming strange force fields and strange signal processing. You have a choice. There is a great chasm. It is a binary choice. You cannot do it a fuzzy way. Either you give up on these phenomena—you give up on all that stuff—or else you have to open yourself up to really crazy things, much more than just quantum theory.

Radin (1997) also addressed the issue of future models involving Group B anomalies thusly:

> As some of the stranger aspects of quantum mechanics are clarified and tested, we're finding that our understanding of the physical world is becoming more compatible with psi. An adequate theory of psi, however, will almost certainly not be quantum theory as it is presently understood. Instead, existing quantum theory will ultimately be seen as a special case of how nonliving matter behaves under certain circumstances. Living systems may require an altogether new theory. Quantum theory says nothing about higher-level concepts such as meaning and purpose, yet real-world, "raw" psi phenomena seem to be intimately related to these concepts.

We particularly resonate with the view of Radin (1997) that QM will ultimately be shown to be a special case of a much broader theory yet to be fully revealed but one that applies to all matter, living and non-living. We think that particle–wave duality, discovered by physicists of the last century, will ultimately be seen as the "shadow" cast into spacetime from the higher dimensional non-spacetime domains.

Getting back to our earlier experimental work (Tiller, Dibble, & Kohane, 2001, Tiller, Dibble, & Fandel, 2005, Tiller, 2007, Tiller, *White Paper XIII*), we discovered the presence of many different types of anomalies that ultimately deserve serious attention but are beyond the scope of this paper (Tiller & Dibble, 2001). However, two major anomalies associated with large values of α_{eff} should at least be mentioned here. These are (1) the DC magnetic field polarity effect (Tiller, Dibble, & Kohane, 2001:173, 206–216) which is consistent with "lifting" an experimental space from the U(1) electromagnetic (EM) Gauge symmetry state (designated by us as the uncoupled state of physical reality) to the SU(2) EM Gauge symmetry state (Tiller, 2007:71–72) (designated by us as the coupled state of physical reality) and (2) the presence of very low frequency oscillations (10^{-1} to 10^{-4} Hz) of all property measurements of water

(pH, air temperature, water temperature, and electrical conductivity) (Tiller, Dibble, & Kohane, 2001:176–180, 194–204). Fourier analysis of the oscillation wave shapes show nesting of all the various properties with each other at one physical location and, within one type of property measurement, over separated locations up to 11 feet apart (Tiller, Dibble, & Kohane, 2001:176–180, 194–204). Appendix 4 provides a very brief introduction to Gauge symmetry state considerations.

In its search to understand nature's manifold expressions, since the days of Decartes 400 years ago, orthodox science has utilized a distance–time-only reference frame (RF) for its investigations and has sought for internal self-consistency over a very large body of diverse phenomena relative to this RF. This has been a very successful strategy! However, natural phenomena such as consciousness, intention, emotion, mind, spirit, love, parapsychology, etc., do not appear to be distance/time-dependent, at least not the same way that the main body of this ~400 year long record of data-gathering has proved to be. Clearly, this tried-and-true RF used for today's paradigm of quantum mechanics and relativistic mechanics is inadequate to handle this other large category of natural phenomena. Further, when one is considering complex living biological systems such as humans and other vertebrates, a mix of these two uniquely different classes of phenomena are entangled while serving the overall life process. All such systems must be considered as anomalous phenomena relative to today's orthodox paradigm and RF. Under such a circumstance, the word *anomalous* loses its meaning and signals that it is time for an RF change.

Another key piece of understanding needed for readers of this paper is the relationship between the $\alpha_{eff} = 0$ condition to the uncoupled state of physical reality also given as the U(1) electromagnetic (EM) gauge symmetry state, our present-day normal reality. Also, the $0 < \alpha_{eff} < 1$ condition is the partially coupled state of physical reality, designated as the SU(2) EM gauge symmetry state. The letters, here, are from group theory notation, while the numbers refer to how many independent phase angles exist in that particular gauge state (Tiller & Dibble, 2007).

In Tiller, Dibble, and Fandel (2005:89–91), our studies strongly suggested that the human acupuncture meridian system is always functioning at a partially coupled state of physical reality with an $\alpha_{eff} > 0$. Thus, highly inner-self–managed humans, who have seriously practiced "inner-work," are also able to "condition" a space by their own intentions and create a local $\alpha_{eff} > 0$ so that local anomalies can occur just as occurs with our IHDs.

The upshot of all this is that there are many origins for anomalous phenomena present in Equation 1. Clearly, all contributions of the $\alpha_{eff} Q_m$ type are anomalous because they originate from what one would label higher dimensional domains of reality than those investigated with today's distance–time

only investigative tools (Q_e-type tools). Some purely Q_e-type phenomena may be considered to be anomalous because they behave in ways unexpected by orthodox science and need to be studied more thoroughly before one can see internally self-consistent connections to other well-known and already accepted distance–time dependent phenomena (Tiller & Dibble, 2007). An example that falls into this category would be a natural phenomenon that is an unappreciated member of a set of Onsager relationship systems. Here, the more complex do the force interconnections between various distance–time-dependent phenomena become, the more easily can a term or terms in a larger Onsager system matrix be misinterpreted.

Summary

In summary, we clearly believe that anomalies research is all about first finding good controls. This belief is fundamentally rooted in an understanding of Equation 1 and its implications. Without good controls, nothing quantitative can be said about any anomalous results. That having been said, one needs to realize what all the impediments are to finding good controls. The very nature of an "anomalous space" itself is one of these impediments. The particular qualities of these spaces produce entanglement effects that significantly complicate matters. An understanding of these effects is crucial to proper anomalies research, and we believe this communication is a step toward this goal.

References

Atmanspacher, H. (2009). Scientific research between orthodoxy and anomaly. *Journal of Scientific Exploration, 23*(3), 273–298.

Jahn, R. G., & Dunne, B. J. (2008). Change the rules! *Journal of Scientific Exploration, 22*(2), 193–213.

Moriyasu, K. (1983). *An Elementary Primer for Gauge Theory.* Singapore: World Scientific Publishing.

Pajunen, G. A., Purnell, M. J., Dibble, W. E., Jr., & Tiller, W. A. (2009). Altering the acid/alkaline balance of water via the use of an intention-host device. *Journal of Alternative and Complementary Medicine, 15,* 963–968.

Radin, D. (1997). *The Conscious Universe: The Scientific Truth of Psychic Phenomena*. New York: HarperEdge.

Stumm, W., & Morgan, J. J. (1996). *Aquatic Chemistry, Chemical Equilibria, and Rates in Natural Waters*, 3rd edition. New York: John Wiley & Sons. 1,022 pp.

Sturrock, P. A. (2007). The role of anomalies in scientific research. *Journal of Scientific Exploration, 21*(2), 241–260.

Tiller, W. A. *White Paper XIII*. All of our publications in the psychoenergetics science area are listed in White Paper XIII of author Tiller's website, http://www.tiller.org

Tiller, W. A. (1997). *Science and Human Transformation: Subtle Energies, Intentionality and Consciousness*. Pavior Publishing.

Tiller, W. A. (2007). *Psychoenergetic Science: A Second Copernican-Scale Revolution*. Pavior Publishing.

Tiller, W. A. (2010a). On understanding the very different science premises meaningful to CAM vs.

orthodox medicine: Part I, The fundamentals. *Journal of Alternative and Complementary Medicine, 16,* 327–335.

Tiller, W. A. (2010b). On understanding the very different science premises meaningful to CAM vs. orthodox medicine: Part II, Applications of Part I fundamentals to five different space–time examples. *Journal of Alternative and Complementary Medicine, 16,* 507–516.

Tiller, W. A., & Dibble, W. E., Jr. (2001). New experimental data revealing an unexpected dimension to materials science and engineering. *Materials Research Innovations, 5,* 21–34.

Tiller, W. A., & Dibble, W. E., Jr. (2007). Expanding the thermodynamic perspective for materials in SU(2) electromagnetic (EM) gauge symmetry state space: Part 1, duplex space model with applications to homeopathy. *Materials Research Innovations, 11,* 163–168.

Tiller, W. A., Dibble, W. E., Jr., & Fandel, G. (2005). *Some Science Adventures with Real Magic*. Pavior Publishing.

Tiller, W. A., Dibble, W. E., Jr., & Kohane, M. (2001). *Conscious Acts of Creation: The Emergence of a New Physics*. Pavior Publishing.

Werbos, P. (2001). What do neural nets and quantum theory tell us about mind and reality? In K. Yasue, M. Jiba, & T. D. Senta (Eds.), *No Matter, Never Mind*, Philadelphia: John Benjamins Publishing Co.

APPENDIX 1
A Brief Sample of Some IHD Research Results

In 1997, we decided to seriously test the unstated assumption of orthodox science, since the days of Descartes, that "no human qualities of consciousness, intention, emotion, mind, or spirit can significantly influence a well-designed target experiment in physical reality." We carefully designed four uniquely different target experiments and a novel procedure for introducing a different specific intention, appropriate to each experiment, after background data had first been gathered on each target experiment. Each of these intention-host device (IHD) experiments was robustly successful (see below) proving unequivocally that, in today's world, this unstated assumption of today's orthodox science is very, very, wrong (Tiller, Dibble, & Kohane, 2001:84–87, Tiller, 2007:67, White Paper XIII).

The intentions for the four target experiments were:

(1) to raise the pH of purified water by 1.0 pH units with no intentional chemical additions to the water,
(2) to decrease the pH of purified water by 1.0 pH units with no intentional chemical additions to the water,
(3) to increase the in vitro thermodynamic activity of a specific liver enzyme, ALP (alkaline phosphatase), by a significant amount via just a 30-minute exposure to an IHD-conditioned space, and
(4) to increase the in vivo ratio of ATP to its chemical precursor, ADP, in the cells of fruit fly larvae by a significant amount and thus significantly reduce the larval development time to the adult fly stage via lifetime exposure of the larvae to an IHD-conditioned space.

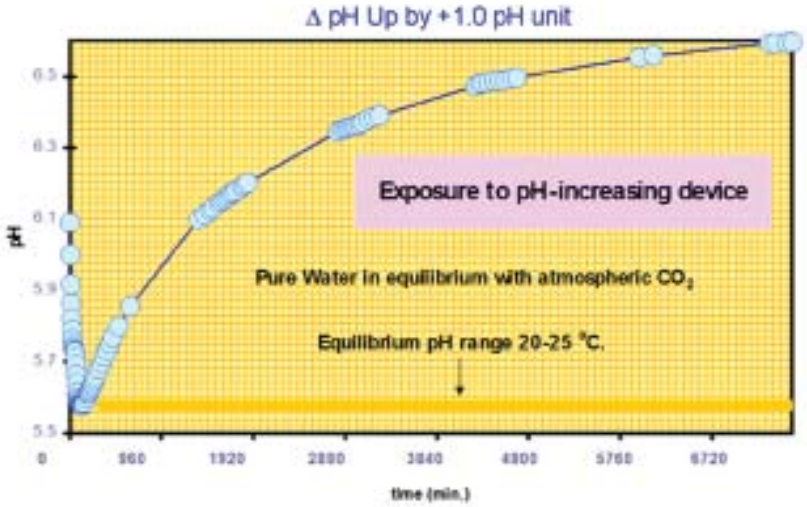

Figure 6. pH vs. time for pH-increasing experiment using an activated IHD.

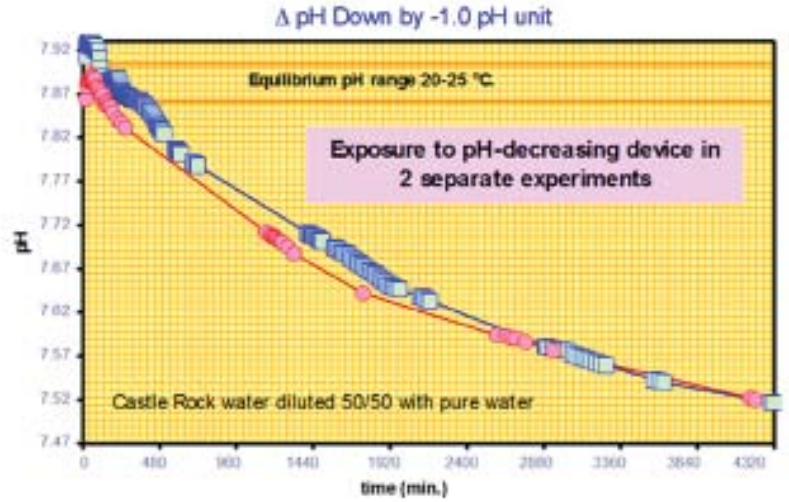

Figure 7. pH vs. time for pH-decreasing experiment using an activated IHD.

Figure 6 and Figure 7 show example results for target experiments (1) and (2) above. For target experiment (3) above, the chemical activity of ALP increased by ~25% − 30% at $p < 0.001$. For target experiment (4), the ATP/ADP

ratio increased by ~10% − 15% at $p < 0.001$, and the larval lifetime decreased by ~20% − 25% at $p < 0.001$.

Intention was added to each experiment via the continuous use of a simple electronic device wherein the specific intention was entangled with the device from a deep meditative state by four highly qualified meditators. Figure 8 illustrates the general time-dependent property measurement change, $Q_M(t)$, with processing time, t, with an activated IHD.

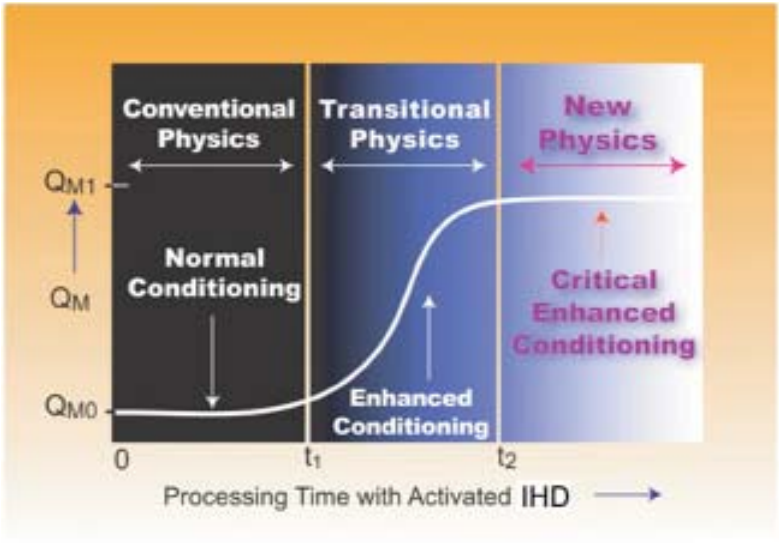

Figure 8. Property measurement change, $Q_M(t)$, vs. processing time, t, using an activated IHD.

APPENDIX 2
Calculation of pH of Purified Water, $pH_{U(1)}$

Since we use the value of $pH_{U(1)}$ as an important control, it is appropriate to discuss how we calculate it. In the main text, the value $pH_{U(1)}$ refers to the value of pH calculated using only thermodynamic data for a given temperature. This calculation assumes that equilibrium has been attained between the purified water and air. We perform this calculation using the four reaction equations discussed below and their equilibrium constants expressed in terms of their temperature dependences.

$$H_2O + CO_2 \Leftrightarrow H_2CO_3(aq). \quad (6)$$

This first equation represents the dissolution of atmospheric CO_2 in water to form carbonic acid (CO_2 dissolved in water or $CO_2(aq)$). The value of the partial pressure of atmospheric CO_2 needed to define the equilibrium constant relation is increasing all the time, the current value being just over 387 ppm. The value used to calculate the pH values, $pH_{U(1)}$, shown in Figure 1, Figure 2, Figure 3, Figure 4, and Figure 5, was 384 ppm, valid in October 2009. The equilibrium constant (simplified) expression for reaction Equation 6 is

$$K_H = [CO_2(aq)/[CO_2(g)]. \quad (7)$$

The second and third equations involve the dissociation of carbonic acid:

$$H_2CO_3(aq) \Leftrightarrow H^+ + HCO_3^- \quad (8)$$

and

$$HCO_3^- \Leftrightarrow H^+ + CO_3^{2-} \quad (9)$$

The corresponding equilibrium constant expressions are

$$K_1 = [H^+] [HCO_3^-] / [CO_2(aq)] \quad (10)$$

and

$$K_2 = [H^+] [CO_3^{2-}] / [HCO_3^-]. \quad (11)$$

The final reaction is the dissociation of water:

$$H_2O \Leftrightarrow H^+ + OH^-, \quad (12)$$

with its equilibrium constant

$$K_w = [H+] [OH-]. \quad (13)$$

The analytical expressions for the temperature dependence for these four equilibrium constants are taken from Stumm and Morgan (1996:979–981). The expression for alkalinity on page 170 of Stumm and Morgan (1996) is then used to calculate the pH at a given temperature. This is possible, assuming the alkalinity of pure water is zero, because the expression then reduces to just values of pH, equilibrium constants (as a function of temperature), and the partial pressure of atmospheric CO_2. The pH is then calculated, iteratively, for a given temperature using the analytical expressions for the temperature dependences for all four equilibrium constants. All these calculations are performed using an Excel spreadsheet.

After a set of pH values for given temperatures is calculated this way, a chart of $pH_{U(1)}$ vs. temperature can be generated. For the temperature range we are normally interested in (16–32 °C), the relationship between pH and temperature calculated this way is nearly linear (goodness of linear fit = 99.95%). This linear relationship is then used to generate the $pH_{U(1)}$ curves of Figure 1, Figure 2, Figure 3, Figure 4, and Figure 5 using the measured water temperature. This methodology produces the same pH values for pure water that Stumm and Morgan (1996) calculate for rainwater using somewhat different techniques. The pH of rainwater, in equilibrium with the atmosphere, is a little over 5.6 at 20 °C and will continue to drop with time as the partial pressure of CO_2 increases.

Ancillary Issues

There are other gases in air than can influence the pH of the pure water exposed to it but have a negligible effect, compared to CO_2, unless they are artificially enhanced. This must be taken into account in some locations, such as working laboratories or manufacturing facilities, where water-soluble vapors of varying kinds are being produced. The only other caveat is that the pure water used in the measurement be purified to the point that the alkalinity is truly zero.

We prefer pure water as a pH measurement medium because, as shown above, its pH can be independently calculated as a function of temperature. Also the pH will be unaffected by evaporation as long as the evaporation rate is less than the equilibration rate between the water and the air. We facilitate this outcome by using lint-free tissue baffles between the water in a container and the air. If pure water is not used, the pH can be highly sensitive to the concentration of dissolved components (which will change via evaporation).

However, some care must be taken in the experimental measurement of the pH of pure water. High-quality measurement equipment is very important (Pajunen, Purnell, Dibble, & Tiller, 2009). Also we use pH buffers for pH-electrode calibration purposes that have been designed for measuring the pH of very dilute solutions such as pure water. ThermoOrion Pure Water buffers obtained from Fisher Scientific were used for all calibrations. Our common practice is to measure the pH continuously for one week, calibrate the pH-electrode, and then resume measurement using freshly prepared purified water. We feel this will minimize evaporation and possible contamination (dust, insects, etc.) problems but will also lead to a transitory period when the water reacts with the air to establish the equilibrium state for the average temperature. This transition period usually has a duration of 12–24 hours, which means that this early transitory data may not be very useful except possibly to provide some information on the kinetics of the process which can change under conditions where anomalies are present.

APPENDIX 3
One Application of Equation 4 and Equation 5

In our pH-replication experiments (for ΔpH = +1 pH units), we found that they mostly conformed to the equation

$$pH_M(t) = pH_0 + \Delta pH\,(1 - e^{-\beta t}) \tag{14}$$

where $pH_0 = pH_{U(1)}$, provided highly purified water was used, while $\alpha'_{eff} pH_m = \Delta pH\ (1 - e^{-\beta t})$ and ΔpH was approximately the intention value (larger for below-ground sites and smaller for several stories' above-ground sites). In this equation, β is a constant, with respect to time, often determined by curve-fitting techniques, and t represents time.

From Equation 5,

$$\frac{dQ_m}{dk_t} = I(k_t) = g(k_t)g^*(k_t) \quad , \qquad (15)$$

where

$$g(k_t) = R(k_t)e^{i\theta(k_t)} \quad . \qquad (16)$$

Here, $g(k_t)$ is a vector of amplitude $R(k_t)$ and phase angle $\theta(k_t)$ with $i = \sqrt{-1}$. Also, k_t is a coordinate in frequency space (R-space) that has as analogues in direct space (D-space) the four coordinates x, y, z, t. Thus, k_t represents one of the frequency domain coordinates, k_x, k_y, k_z, and k_t, which are all spatial or temporal frequencies. In Equation 15, $I(k_t)$ is the intensity value analogous to a magnitude but in the frequency domain.

In the zeroth-order approximation, Equation 4b yields

$$g(k_t) = \frac{-\alpha'_{eff} pH_0}{(2\pi)^{3/2} ik_t}\left(1 - e^{-i2\pi tk_t}\right) \quad . \qquad (17)$$

Thus, from Equation 2 and Equation 14,

$$Q_m = \frac{\Delta pH}{\alpha'_{eff}}(1 - e^{-\beta t}) \quad , \qquad (18)$$

so that

$$\frac{dQ_m}{dk_t} = \frac{\Delta pH}{\alpha'_{eff}} te^{-\beta t} \frac{d\beta}{dk_t} = g(k_t)g^*(k_t)$$

$$= \frac{\left(\alpha'_{eff} pH_0\right)^2}{(2\pi)^3 k_t^2}\left(1 - e^{+i2\pi k_t t}\right)\left(1 - e^{-i2\pi k_t t}\right)$$

$$= \frac{\left(\alpha'_{eff} pH_0\right)^2}{(2\pi)^3}\left[\frac{2 - \left(e^{+i2\pi k_t t} + e^{-i2\pi k_t t}\right)}{k_t^2}\right] \qquad (19)$$

$$= \frac{2\left(\alpha'_{eff} pH_0\right)^2}{(2\pi)^3}\left[\frac{1 - \cosh\left(i2\pi k_t t\right)}{k_t^2}\right]. \qquad (20)$$

From Equations 19 and 20,

$$e^{-\beta t}\, d\beta = a\left[\frac{1-\cosh(bk_t)}{k_t^2}\right] dk_t \tag{21}$$

where

$$a = \frac{2\left(\alpha'_{eff}\right)^3 \left(pH_0\right)^2}{(2\pi)^3\, t\Delta pH} \quad \text{and b= } 2\pi it. \tag{22}$$

Integrating Equation 21 yields

$$e^{-\beta t} = a' \int \left[\frac{1-\cosh(bk_t)}{k_t^2}\right] dk_t \tag{23}$$

where

$$a' = -ta = \frac{-2\left(\alpha'_{eff}\right)^3 \left(pH_0\right)^2}{(2\pi)^3\, \Delta pH} \,. \tag{24}$$

Experimentally, we find that each different site has a different value of β so that exploring the details of Equation 23 and Equation 24 can be expected to yield interesting relationships between the two reciprocal subspaces. In particular, one readily obtains an explicit expression for $(\alpha'_{eff})^3$ given by

$$\left(\alpha'_{eff}\right)^3 = \frac{-(2\pi)^3 \Delta pH e^{-\beta t}}{2(pH_0)^2 \int \left[\frac{1-\cosh(bk_t)}{k_t^2}\right] dk_t} \quad . \qquad (25)$$

Since cosh(ix) = cos(x) with $x = 2\pi t k_t$, Equation 25 becomes

$$\left(\alpha'_{eff}\right)^3 = \frac{-(2\pi)^2 \Delta pH e^{-\beta t}}{(pH_0)^2 \int_{2\pi t k_t^*}^{2\pi t k_t^{**}} \left(\frac{1-\cos(x)}{x^2}\right) dx} \quad . \qquad (26)$$

In the small limit approximation, $0 \leq x < 2$, the integral is better than 90% accurate when one expresses the cosine as a power series. Of course, at large x, the integral rapidly shrinks to ~zero. Because of the negative sign, one must expect that α'_{eff} is mathematically complex in nature and can be quantitatively evaluated.

APPENDIX 4
A Brief Synopsis on Gauge Theory

Gauge theory development has probably been the most important advance in orthodox physics in the past 50 years. It deals with the interaction of external fields with internal symmetry states in nature (Moriyasu, 1983).

It deals with dynamic movement, in phase space, of the electron wave function phase angle, θ, with respect to the absence or detailed presence of an external field and the particular Gauge symmetry state that the electron may occupy. This is dependent on fiber bundle mathematics and group theory considerations leading to a unique locus of the particle's phase angle, θ, at each (x,y,z,t) point in spacetime. Our normal macroscopic physical reality exists in a U(1) gauge symmetry state because it involves only one type of relevant particle, the electron, whose phase angle, θ, moves in a planar ring in phase space

(see Figure 9). The SU(2) Gauge state involves two relevant phase angles, θ and ϕ, which move in a three-dimensional sphere in phase space at each (x,y,z,t) point as indicated in Figure 9.

For SU(n) Gauge states, $n^2 - 1$ parameters are involved in the relevant interaction so that, for n = 2, three parameters are critically involved. Thus, for the neutron/proton exchange reaction, this is an SU(2) Gauge state with the neutrino as the third parameter. In the case of an electron/magnetic monopole interaction it also produces an SU(2) Gauge state. What WAT has labeled a "deltron" is the third parameter needed to stabilize this particular symmetry state. Loss of the deltron from this complex leads to symmetry breaking from the self-coherent state to the free state (see Figure 9) and transition to a U(1) Gauge state for the electron plus a different type of U(1) Gauge state for the magnetic monopole (but undetectable via our orthodox spacetime instrumentation). A greatly expanded version of Gauge symmetry theory is provided in White Paper XIX available at http://www.tiller.org.

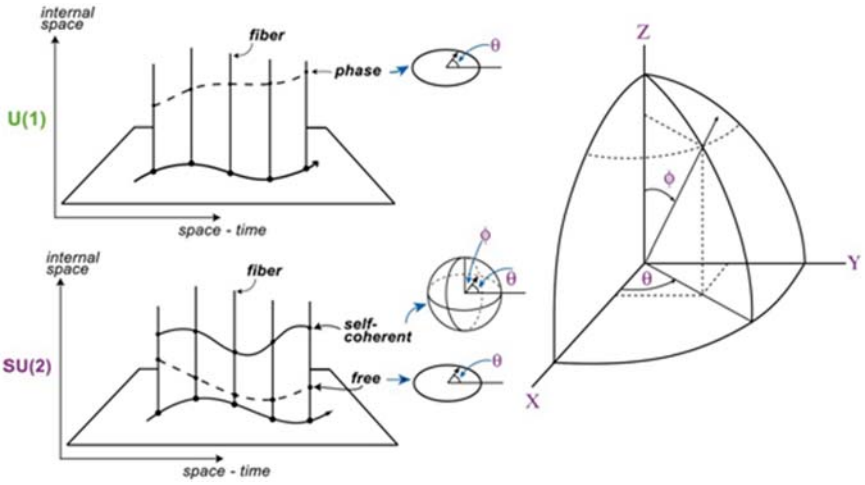

Figure 9. Fiber bundle representation above the spacetime background for both U(1) and SU(2) gauge symmetry states.